International Journal of Modern Physics B, Vol. 7, Nos. 9 & 10 (1993) 1779–1788

GRANULAR MEDIA ON A VIBRATING PLATE: A MOLECULAR DYNAMICS SIMULATION

JASON A.C. GALLAS, HANS J. HERRMANN and STEFAN SOKOŁOWSKI
Höchstleistungsrechenzentrum, KFA, D-5170 Jülich, Germany.

When sand or other granular materials are shaken, poured or sheared many intriguing phenomena can be observed. We will model the granular medium by a packing of elastic spheres and simulate it via Molecular Dynamics. Dissipation of energy and shear friction at collisions are included. The onset of fluidization can be determined and is in good agreement with experiments. On a vibrating plate we observe the formation of convection cells due to walls or amplitude modulations. Density and velocity profiles on conveyor belts are measured and the influence of an obstacle discussed. We mention various types of rheology for flow down an inclined chute or through a pipe and outflowing containers.

1. Introduction

We consider in this paper some of the many astonishing phenomena that can be observed when granular materials like sand or powder move[1–2]. *Standard* examples are the so-called "Brazil nut" segregation[3–5], heap formation under vibration[6–8], density waves emitted from outlets[9] and 1/f noise in the power spectra local forces[10]. All these effects eventually originate from the fact that granular materials form a hybrid state between a fluid and a solid: When the density exceeds a certain value, the critical dilatancy[11,12], it is resistant to shear, like solids, while below this density it will "fluidify". In contrast to usual fluids, granular materials might also display stable density waves. Their presence in fact complicates the characterization and study of "fluidized states".

There have been so far many attempts to formalize and quantify the complicated rheology of granular media. Continuum equations of motion[13], a cellular automaton[14] and a random walk approach[15] have been proposed. But most of the aforementioned effects have not been so far satisfactorily explained by these techniques. Molecular Dynamics simulations seem to be a good tool to study these phenomena in more detail. It is important to observe that molecular dynamics has already been used to investigate several aspects of granular media. For an extensive

bibliography see please ref. 2.

Particularly suited to study fluidization is an experiment where sand is put on a loudspeaker or on a vibrating table[6–8,16–18]. Under gravity the sand jumps up and down and although kinetic energy is strongly dissipated, collisions among the grains reduce its density thereby allowing it to flow ("fluidization"). Under certain circumstances flow between top and bottom can occur in form of convection cells as has been observed experimentally in the case of inhomogeneities in the amplitude of the vibration [19]. Also within the heaps[6–8] convection occurs and might even be the motor for the heap formation. When the vibration of the plate also has a horizontal component the material will flow in one direction, a technique often used in powder transport.

In this paper we discuss Molecular Dynamics (MD) simulations of inelastic particles with an additional shear friction performed for two-dimensional systems. We discuss data for the onset of fluidization[16] and give evidence for the occurence of convection cells due to inhomogeneities in the vibration amplitude or due to walls, an effect that has also been observed recently[20,21]. We also report on measurements of the velocity and density profiles of powder transported on a vibrating belt[22]. In fact, MD simulations[23,24] have already been applied to granular media to model segregation[5], outflow from a hopper[25,26], shear flow[27] and flow down an inclined chute[28].

2. Model

We consider a system of N spherical particles of equal density and with diameters d chosen randomly from a homogeneous distribution of width w around $d_0 = 1$ mm. These particles are placed into a container of width L that is open on the top and has either periodic boundary conditions or fixed walls in the horizontal direction. When two particles i and j overlap (i.e. when their distance is smaller than the sum of their radia) three forces act on particle i: 1.) an elastic restoration force

$$\vec{f}_{el}^{(i)} = Y m_i(\mid \vec{r}_{ij} \mid -\frac{1}{2}(d_i + d_j))\frac{\vec{r}_{ij}}{\mid \vec{r}_{ij} \mid} \quad , \tag{1a}$$

where Y is the Young modulus (normalized by the mass), $m_i \propto d_i^2$ the mass of particle i and $\vec{r}_{ij}$ points from particle i to j; 2.) a dissipation due to the inelasticity of the collision

$$\vec{f}_{diss}^{(i)} = -\gamma m_i(\vec{v}_{ij} \cdot \vec{r}_{ij})\frac{\vec{r}_{ij}}{\mid \vec{r}_{ij} \mid^2} \quad , \tag{1b}$$

where γ is a phenomenological dissipation coefficient and $\vec{v}_{ij} = \vec{v}_i - \vec{v}_j$ the relative velocity; 3.) a shear friction force that mimics to some degree the effect of solid friction

$$\vec{f}_{shear}^{(i)} = -\gamma_s m_i(\vec{v}_{ij} \cdot \vec{t}_{ij})\frac{\vec{t}_{ij}}{\mid \vec{r}_{ij} \mid^2} \quad , \tag{1c}$$

where γ_s is the shear friction coefficient and $\vec{t}_{ij} = (-r_{ij}^y, r_{ij}^x)$ is the vector $\vec{r}_{ij}$ rotated by 90°. As compared to other modelizations of the forces acting between grains[5,25,27,29,30] our eqs. 1 are simpler since we neglect Coulomb friction and the rotation of particles. In fact, solid friction should be proportional to the normal force but the term of eq. (1c) is always needed to halt the tangential relative motion[29]. We did these simplifications on purpose in order to have less, in our opinion unimportant, fit parameters. In fact, under realistic deviations from the spherical shape of the particles rotations are strongly suppressed.

When a particle collides with a wall the same forces act as if it would have encountered another particle of diameter d_0 at the collision point. Two forces act on the system, on one hand gravitation $g \approx -10\text{m/s}^2$ pulls each particle down, on the other hand the bottom of the container is subjected to a vibrating motion described by:

$$z_0(t) = A(x)\sin(2\pi f t) \quad , \tag{2}$$

f being the frequency and amplitude A. In some aplications we will consider an explicit spatial modulation of A of the form

$$A(x) = A_0(1 - B\cos(2\pi x/L)) \quad . \tag{3}$$

For vibrating conveyor belts the bottom "plate" undergoes harmonic oscillations in both horizontal (x) and vertical (z) directions according to

$$x(t) = A_x\sin(2\pi f t) \quad and \quad z(t) = A_z\sin(2\pi f t) \tag{4}$$

where f is the frequency and A_x and A_z are x and z amplitudes, respectively. The corresponding angle of the composed oscillation is $\alpha = \arctan(A_z/A_x)$.

Two initial positions of the particles are considered: they are either placed regularly on the bottom of the container or put at random positions inside a space several times as high as the dense packing. The initial velocities are either zero or randomly chosen. After that the particles are allowed to fall freely under gravity and relax for a time that corresponds to ten or twenty cycles of the vibration. The displacements, velocities and energies are then measured by averaging over up to 200 cycles. We use a fifth order predictor-corrector MD with $2 - 6 \times 10^4$ iteration steps per cycle which vectorizes on the Cray Y-MP running at about 10 μsec per particle-update on one processor and simulating up to 2000 particles. The program was also implemented on eight processors of the Intel hypercube with a speed of about 3×10^4 updates per second by cutting the system into slices. Each slice was then treated by one i860 processor interchanging particle positions via message passing[31].

3. Results

A recent paper[17] reported experimental observations of a "fluidized" state in a 2D vertical packing of steel spheres submitted to vertical vibrations. They shake periodically (at $f = 20Hz$) 300 steel beads inside a trapezoidal cell. Positions and

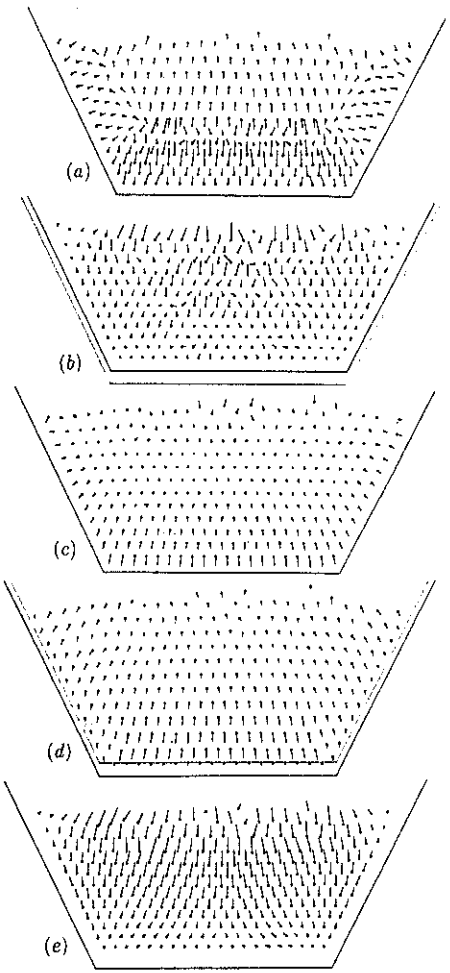

Fig. 1. Instant positions (center of circles) and velocities (represented by line segments emerging form the beads) for the phase φ equal to (a) $\pi/2$; (b) π; (c) $3\pi/2$; and (d) 0. In (e) the center of the circles are the positions at $\varphi = 0$ while the end of the line segments show the positions at 15 ms later. A few beads undergoing ballistic flights are not shown.

velocities of the particles were obtained. We did simulations[16] of precisely the same geometry and number of particles as in the experiment[17].

Figures 1a-d show snapshots taken at four different phase-values of the oscillation, namely, $\varphi = \pi/2$, π, $3\pi/2$ and 0, where $\varphi = 2\pi ft$. The solid lines represent

the actual position of the cell while dotted boxes stand for their starting position at $\varphi = 0$. The dots inside represent bead positions while the line segments emerging from them represent *instant velocities*. By comparing Figs. 1a-d among each other it is possible to reconstruct the motion of the beads during a full cycle of the shaking. Starting at $\varphi = 0$, the bottom of the cell goes up, thereby transfering momentum to the spheres. One can see that there is a delay in the transmission of the momentum to the top layers as one might intuitively expect. In Fig. 1a the cell is at the highest possible position and starting to reverse its movement. Note that the particles at the top still have enough velocity to keep going up. Figure 1e is intended to be our equivalent of Fig. 1 of Clement and Rajchenbach[17]. Dots still represent positions of the spheres at $\varphi = 0$ but now the end of the line segments indicate *positions* of the particles at a time $t = 15$ ms later. From such snapshots it is easy to realize that while movement of "computer" spheres is rather symmetric with respect to a reflection about a vertical line passing through the center of the cell, the corresponding experimental picture obtained by Clement and Rajchembach is not so. We attribute such differences to small uncontrolable non-uniformities in the experimental setup.

To check whether the present model is at all able to display a transition from a solid- to a fluid-like state we varied both frequency f and amplitude A of the oscillations. We recorded the trajectory of a selected "tracer" particle, and monitored its motion as time evolved. In the solid-like case the tracer particle remains confined to a very small region while in the fluid-like case the trajectory seems to explore the entire box. It is important to note that both situations can occur for the same value of Af^2 which means that, contrary to widespread believe, Af^2 is not a good scaling variable even close to the onset of fluidization. As more extensively discussed in ref. 16, our simulations reproduced quantitatively quite well the experimental data reported in ref. 17.

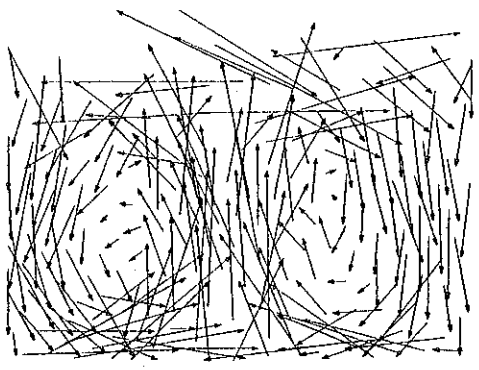

Fig. 2. Displacement of the particles after 15 cycles for $f = 70$Hz using 200 particles in a box with periodic boundary conditions of size $L/d_0 = 20$ with $A_0 = 1.5d_0$, $B = 0.5$, $w = 0.5$, $Y = 5000/d_0$, $\gamma = 20g$ and $\gamma_s = 400/f$.

Next we considered the case of a spatial modulation in the amplitude of the vibration, i.e. $B \neq 0$ in eq. (3), using periodic boundary conditions.[20] In Fig. 2 we see the displacements of the particles after 15 cycles for $B = 0.5$. Clearly the particles flow upwards in the center where the amplitude of the vibration is larger and form two convection cells. If the dissipation coefficient γ is increased by a factor of ten the convection is completely suppressed while it is quite insensitive to γ_s, even if $\gamma_s = 0$. The elastic modulus also has only a very weak influence as long as it remains larger than 10^3 (in units of d_0). The initial condition plays no noticeable effect showing that convection is no transient effect. The polydispersity w of the particles only slightly distorts the shape of the convection cells.

The strength of the convection was measured quantitatively by recording the average vertical components of the velocities of the particles in the center and at the edges. These quantities have also been measured experimentally by Rátkai[19]. The strongest convection for the aforementioned parameters is obtained around 60 Hz and it increases dramatically with the amplitude A_0 as was also seen in the experiment[19]. This resonance seems to be the driving force of the convective motion.

A completely different type of convection can be caused by the existence of fixed vertical walls without any spatial modulation of the amplitude[20], i.e. for $B = 0$ in eq. (3). One sees in Fig. 3 for $\gamma_s = 0$ convection cells where the motion of the particles at the wall is upward. On the other hand, when $\gamma_s \neq 0$ there is at each wall a very strong downward drag giving rise to a convection in the opposite sense. When the cell is made larger the two convection cells remain attached to the walls showing that the walls are at the origin of these cells. One also recognizes a slight heap formation close to the wall which might be a first sign of the famous sand heaps discovered by Faraday[6–8].

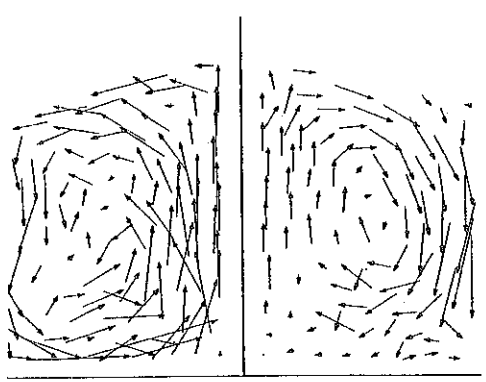

Fig. 3. Displacements after 20 cycles in a system with fixed vertical walls for $B = 0$, $w = 0.5$, $Y = 5000/d_0$, $f = 20$Hz, $N = 200$, $L = 20d_0$, $A_0 = 2.0\ d_0$, $\gamma = 80g$, $\gamma_s = 0$.

Let us next discuss the behaviour of vibrating conveyor belts[22], i.e. granular material under harmonic vibrations having a given angle with respect to the direction of gravity as described in eq. (4). Vibrating conveyor belts as a means of transportation are very typical for granular media, since neither solids nor fluids can be moved on them and are used for instance in the pharmaceutical industry to transport pills [32].

We measured density and velocity profiles as a function of height z in the steady state. Close to the belt the local density is very small, then it has a maximum and at large heights it falls off. Only at low frequency the local density shows a plateau extending up to larger z values. When the frequency increases, the maximum of the local density decreases and the density profile smears out. The tail at large heights indicates the existence of particles in a gas-like state above the free surface of the packing. The density profile is rather independent on the angle of vibrations which means that the vertical component of the vibration determines almost completely the vertical density of the beads. When the friction coefficients decrease, the system becomes more gas-like. Only very close to the belt the profiles seem independent on the friction. The velocity profiles exhibit a well-developed plateau, showing that almost all particles move at the same speed. Obviously, the velocity increases with increasing frequency and decreasing angle of vibrations and for $\gamma_s = 0$ the velocity is zero. For $\gamma_s \geq 50g$ the velocity profile depends only very weakly on the shear friction coefficient.

Let us consider the trajectories of the particles during one cycle of shaking. When the frequency is low enough all the beads move synchronously along elliptic trajectories. The tilting angle of these ellipses increases with the angle of vibrations. For smaller shear friction coefficients γ_s the tilting angle tends to $\pi/2$, provided the vibration frequency is low enough. When the beads start to flow, the character of their trajectories changes: at not too high frequencies they move along sinusoidal curves. With increasing frequency, the trajectories become flatter and at the highest frequencies we observe a nearly horizontal flow (see Fig. 4a). A decrease of the vibration angle makes the horizontal motion more pronounced. A similar effect occurs when the friction coefficients are increased. For vanishing shear friction γ_s the beads move essentially vertically.

Next we checked how a circular obstacle inserted into the system influences the flow. To this end, a fixed circular body was inserted at $x_1 = L/2$, $z_1 = A_z$. The diameter of this obstacle was varied from $d_1 = 0.1d_0$ to $d_1 = 2.5d_0$. The parameters characterizing the interactions of the obstacle with the particles were the same for particle-particle interactions. Note that due to the periodic boundary conditions, the obstacle is repeated along the belt. Even the presence of a rather small obstacle rapidly slows down the flow. In Fig. 4b we see the trajectories of the particles for an obstacle of $d_1 = 1.5d_0$ with the same parameters as in Fig. 4a. Clearly the presence of the obstacle changes the trajectories of all the particles considerably. So, we cannot treat the obstacle as only locally influencing the flow, because the stiff repulsion between particles generates long-range correlations.

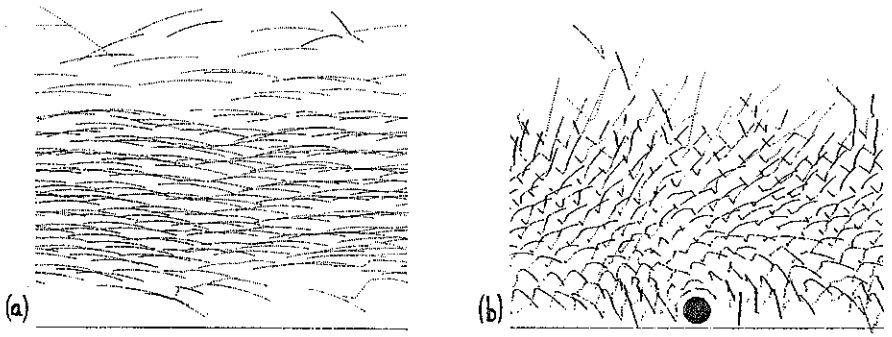

Fig. 4. Trajectories of the particles in steady state during a single cycle. The position of each particle is plotted after every 50 iteration steps. The plots were obtained for $A_z = d_0$, $\alpha = \pi/4$, $\gamma = \gamma_s = 50g$ and $f = 80$ Hz. (a) without and (b) with an obstacle of diameter $d_1/d_0 = 1.5$ given by the full circle.

Using similar techniques but including the Coulomb (dynamic) friction and rotations of particles as in[5] new simulations were made recently for the flow out of a hopper[25], flow down an inclined chute[28] and flow through a pipe[33]. Because of the lack of static friction the simulations of the hopper have not reproduced the observed density waves[9] but nevertheless they find the existence of a minimal outlet diameter due to some kind of arching which is larger for equal sized particles than for randomly distributed radia. The simulations down an inclined plane very accurately reproduce the various types of flow and the dependence of the velocity profile on the smoothness of the plane as they were observed in recent experiments[34]. Flow through a vertical pipe with rough walls[33] was found to generate density waves. Their appearance and speed strongly depends on small details of the initial positions of the grains. The similarity to the experimental situation was illustrated in a movie shown at this conference. Including also the static friction into the simulation as in ref. 29, heaps and avalanches were obtained and various characteristic angles (repose, minimal stability, tilting) were measured[30].

4. Conclusion

Using a rather simple two-dimensional model of an ensemble of inelastic spherical particles with shear friction we have shown that many interesting rheological properties of granular materials can be reproduced. Not only relative magnitudes of friction forces play a decisive role but constraints and boundary conditions have also a great impact on the possible dynamical behavior observed. Various types of convection can occur on a vibrating plate and density waves appear during the flow through a pipe. We illustrated these simulations in a movie. Three dimensional

simulations should also be performed but it is difficult to treat systems large enough to ensure the reliability of the results.

Acknowledgements

We thank J. Lee, C. Moukarzel, T. Pöschel and G. Ristow for many enlightening discussions. JACG thanks the Brazilian agency CNPq for partial support.

References

1. H.M. Jaeger and S.R. Nagel, Science **255**, 1523 (1992)
2. (a) S.B. Savage, Adv. Appl. Mech., **24**, 289 (1984); C.S. Campbell, Annu. Rev. Fluid Mech. **22**, 57 (1990); (b) H.J. Herrmann, in "Disorder and Granular Media", eds. D. Bideau and A. Hansen (North-Holland, Amsterdam, 1993).
3. J.C. Williams, Powder Techn. **15**, 245 (1976)
4. A. Rosato, K.J. Strandburg, F. Prinz and R.H. Swendsen Phys.Rev.Lett. **58**, 1038 (1987)
5. P.K. Haff and B.T. Werner, Powder Techn. **48**, 239 (1986)
6. M. Faraday, Phil. Trans. R. Soc. London **52**, 299 (1831)
7. P. Evesque and J. Rajchenbach, Phys. Rev. Lett. **62**, 44 (1989)
8. J. Walker, Sci. Am. **247**, 167 (1982)
9. G.W. Baxter, R.P. Behringer, T.Fagert and G.A. Johnson, Phys. Rev. Lett. **62**, 2825 (1989)
10. C.-h. Lui and S.R. Jaeger, Phys. Rev. Lett. **68**, 2301 (1992); G.W. Baxter, PhD thesis
11. O. Reynolds, Phil. Mag. S. **20**, 469 (1885)
12. Y.M. Bashir and J.D. Goddard, J. Rheol. **35**, 849 (1991)
13. S.B. Savage, J. Fluid Mech. **92**, 53 (1979)
14. G.W. Baxter and R.P. Behringer, Phys. Rev. A **42**, 1017 (1990), Physica D **51**, 465 (1991)
15. H. Caram and D.C. Hong, Phys. Rev. Lett. **67**, 828 (1991)
16. J.A.C. Gallas, H.J. Herrmann and S. Sokolowski, Physica A, **189**, 437 (1992).
17. E. Clement and J. Rajchenbach, Europhys. Lett. **16**, 133 (1991)
18. O. Zik, J. Stavans and Y. Rabin, Europhys. Lett. **17**, 315 (1992)
19. G. Rátkai, Powder Techn. **15**, 187 (1976)
20. J.A.C. Gallas, H.J. Herrmann and S. Sokołowski, Phys. Rev. Lett., **69**, 1371 (1992).
21. Y-h. Taguchi, Phys. Rev. Lett. **69**, 1367 (1992).
22. J.A.C. Gallas, H.J. Herrmann and S. Sokolowski, J. Physique II, **2**, 1389 (1992)
23. M.P. Allen and D.J. Tildesley, *Computer Simulation of Liquids*, Oxford University Press, Oxford, 1987
24. D. Tildesley, in *Computational Physics*, edited by R.D. Kenway and G.S. Pawley, NATO Advanced Study Institute, Edinburgh University Press, 1987
25. G. Ristow, J. Physique I **2**, 649 (1992)
26. D.C. Hong and J.A. McLennan, Physica A **187**, 159 (1992)

27. C.S. Campbell and C.E. Brennen, J. Fluid Mech. **151**, 167 (1985); P.A. Thompson and G.S. Grest, Phys. Rev. Lett. **67**, 1751 (1991); O.R. Walton and R.L. Braun, J. Rheol. **30**, 949 (1986)
28. T. Pöschel, preprint HLRZ 22/92, to appear in J. Physique, Paris.
29. P.A. Cundall and O.D.L. Strack, Géotechnique **29**, 47 (1979)
30. J. Lee and H.J. Herrmann, preprint HLRZ 44/92
31. G. Ristow, preprint HLRZ 48/92
32. H. Schmidt and I. Peschl, Fördern u. Heben **15**, 606 (1965)
33. T. Pöschel, preprint; T. Pöschel and J.A.C. Gallas, preprint.
34. T.G. Drake , J. Geophys. Res. **95**, 8681 (1990)